J|A|C|S COMMUNICATIONS

Published on Web 06/29/2010

Organic Two-Step Spin-Transition-Like Behavior in a Linear $S = 1$ Array: 3′-Methylbiphenyl-3,5-diyl Bis(*tert*-butylnitroxide) and Related Compounds

Hirokazu Nishimaki and Takayuki Ishida*

Department of Engineering Science, The University of Electro-Communications, Chofu, Tokyo 182-8585, Japan

Received April 6, 2010; E-mail: ishi@pc.uec.ac.jp

Abstract: The title compound showed a unique low-dimensional array with $S = 1$ molecules. The intermolecular antiferromagnetic coupling and intramolecular ferromagnetic coupling are simultaneously present, and accordingly, the $S = {}^1/_2$ state appeared at 230−350 K between the diamagnetic phase and the paramagnetic $S = 1$ phase. The solid−solid phase transition occurred in a single-crystal-to-single-crystal manner. The corresponding 3′-methoxy derivative is also presented for comparison.

Solid-sate chromism is of increasing interest for future applications in switching, sensing, memory, display, and other devices.[1] Dithiadiazolyl and dithiazolyl radicals have attracted much attention, as they show various spin structures and physical properties in the solid state on the basis of π dimerization.[2] Phenalenyl radicals have also been studied with respect to their π-dimerization ability even after the introduction of steric protection.[3] There are a few skeletons of organic materials showing facile σ-bond cleavage accompanied by drastic changes in both chromic and magnetic properties [e.g., bis(triarylimidazole)[4] and bis(triaylchromenyl)[5]]. We now add the name of biphenyl-3,5-diyl bis(*tert*-butylnitroxide) (BPBN) to the register of chromic and magnetic materials, but the situation seems somewhat different because the component is a biradical.

The solid−solid phase transition was observed at 350 K for unsubstituted BPBN.[6,7] The $S = 1$ paramagnetic phase originates in the intrinsic high-spin character of each molecule, as in many *m*-phenylene-bridged biradicals.[8] The diamagnetic phase appears when intermolecular antiferromagnetic coupling overwhelmingly surpasses the intramolecular ferromagnetic one. The head-to-tail dimerization found in the crystal structure seems reasonable on the basis of the dipolar character indicated by the contribution of the $N^{+\bullet}-O^-$ moiety. Possible canonical structures are depicted on the left side of Scheme 1a. In short, intramolecular ferromagnetic coupling and intermolecular antiferromagnetic coupling are simultaneously present in a linear array of BPBN. An intermediate $S = {}^1/_2$ phase would be introduced between the $S = 0$ and $S = 1$ phases if the molecular symmetry is lowered and the nitroxide dimerization/degradation takes place in a stepwise fashion (Scheme 1b).

We designed the derivative 3MeBPBN, which is methylated at an asymmetric position on the biphenyl core. This compound was easily prepared[9] according to the Suzuki coupling procedure reported for BPBN[6] by using *m*-tolylboronic acid in place of phenylboronic acid to react with 1,3,5-tribromobenzene. A solution electron spin resonance (ESR) spectrum of 3MeBPBN exhibited a broad singlet, as is typical of BPBN biradicals.[6]

A drastic color change of 3MeBPBN from dark-red [the high-temperature (HT) phase] to light-orange [the low-temperature (LT) phase], as shown in Figure 1, was observed upon cooling. The transition gradually occurred at 230−280 K in a single-crystal-to-single-crystal manner. We could determine the crystal structures

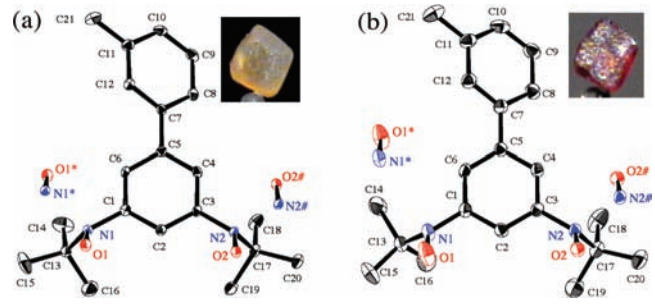

Figure 1. Molecular structures of 3MeBPBN determined at (a) 116 and (b) 296 K with thermal ellipsoids at the 50 and 30% probability levels, respectively. Hydrogen atoms have been omitted. The nearest-neighbor N−O groups are shown, and the symmetry operation codes * and # stand for $-x$, $-y+1$, $-z+1$ and $-x$, $-y$, $-z$, respectively. Only the major conformer is shown in (b). A photo of a single crystal at each temperature is also shown.

Scheme 1. (a) Head-to-Tail Dimerization of Two Adjacent Nitroxides; (b) Three Phases of BPBN Derivatives

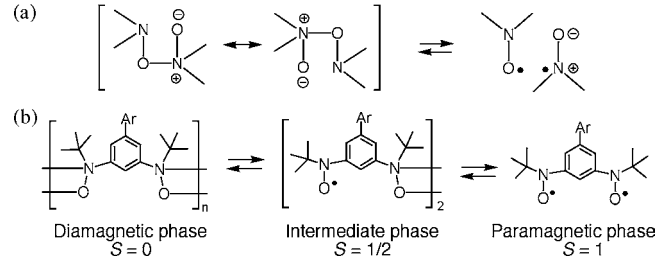

for the two phases,[10] and furthermore, transient structures could be monitored at any given temperature (Figure 1S in the Supporting Information is an animated X-ray crystal structure). Packing of one of the *tert*-butyl groups (on N1) became loose in the HT phase, as indicated by the large thermal displacement factors. This behavior may belong to an order−disorder transition, as a disorder model was successfully applied to the HT phase while no conformer was present in the LT phase. The occupancy factor was optimized to a value of 0.538(16)/0.462(16) for two possible conformers of C14, C15, and C16 at 296 K. On the other hand, the *tert*-butyl group on N2 was packed tightly throughout both phases.

Figure 1 also shows the nearest-neighbor N−O groups in each phase. The crystallographic inversion centers are located at the midpoint of adjacent N−O groups in the $P\bar{1}$ space group; namely, there are double short N···O contacts. The N−O radical groups are separated from each other by 2.379(2) Å for O1···N1* and 2.315(3) Å for O2···N2# at 116 K. These distances are 23−25% shorter than the sum of the van der Waals radii (3.07 Å).[11] At 296 K, the O1···N1* distance is increased [3.686(3) Å] while the O2···N2# distance remains short [2.410(3) Å] (Figure 2 inset). The intramolecular geometries are changed as well. The structure of the C1−N1(−O1)−C13 moiety at 296 K is highly planar for a

10.1021/ja102890g

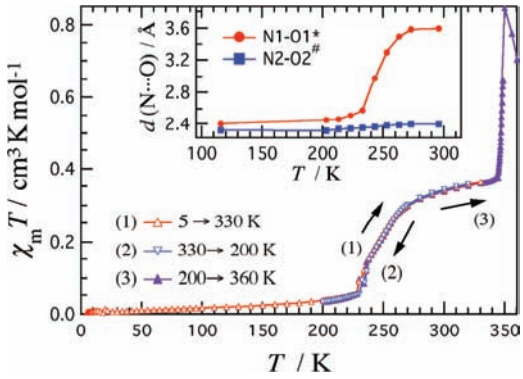

Figure 2. Temperature dependence of $\chi_m T$ for 3MeBPBN measured at 5000 Oe. The solid lines are drawn as guides for the eye. The inset shows the nearest-neighbor interatomic N···O distances as a function of temperature.

normal radical. Strongly dimerized N−O groups have a pyramidalized nitrogen atom (N1 and N2 at 116 K and N2 at 296 K).

We measured the magnetic properties of 3MeBPBN (Figure 2) and clarified an obvious spin-transition-like behavior. The $\chi_m T$ value was practically diamagnetic in the LT phase. When the sample was heated, the $\chi_m T$ value started to increase monotonically from ∼230 K and at ∼300 K reached a plateau of 0.34 cm^3 K mol^{-1}, which approximately corresponds to the theoretical $S = {}^1/_2$ spin-only value (0.375 cm^3 K mol^{-1}). The interconversion was found to be reversible. Further heating caused the $\chi_m T$ value to increase sharply again, reaching 0.84 cm^3 K mol^{-1} at 350 K. This value is larger than the sum of two $S = {}^1/_2$ contributions, indicating that the *intra*molecular ferromagnetic coupling was revived to afford the ground-state $S = 1$ molecules.

The final decrease at 355 K was irreversible and can be ascribed to decomposition of the radical groups. Powder XRD measurements revealed that this temperature was a melting point (Figure 2S). The transition between the $S = {}^1/_2$ and $S = 1$ states was inseparable from the melt. The intramolecular exchange coupling might be evaluated from the population of the triplet state, but the competing decomposition disturbed such a quantitative analysis. Density functional theory molecular orbital (MO) calculations showed that each 3MeBPBN molecule potentially possessed the ground triplet state in any phase (Figure 3S). Intermolecular antiferromagnetic coupling was also confirmed.

The 3′-methyl substitution makes the intermolecular contacts asymmetric. A bulkier substituent would facilitate the cleavage to a greater extent. Thus, we designed and prepared the methoxy derivative 3MeOBPBN.[12] The magnetic study revealed that 3MeOBPBN behaves as an $S = {}^1/_2$ paramagnetic crystalline solid below its melting point (Figure 3). From the crystal structure analysis,[13] a close contact was found on one N−O side, with an N2···O2$^{\#}$ distance of 2.403(3) Å, but there was a somewhat long distance on the other side, with an N1···O1* distance of 5.278(4) Å.

Two-step spin-crossover behavior in iron(II) complexes has been well-investigated in connection with ternary digit information storage and further applications.[1] Similarly, we have exploited here the biradical system showing two-step spin states. It should be noted that BPBN, 3MeBPBN, and 3MeOBPBN are all isomorphous (Figure 4S). We controlled the stability of the three magnetic states by a steric effect: BPBN has only $S = 0$ and $S = 1$ phases, whereas 3MeBPBN exhibits an additional $S = {}^1/_2$ phase and 3MeOBPBN loses the $S = 0$ phase (Scheme 1b).

The present system provides information on any transient form among poly-, di-, and monomeric spin structures in a supramolecular one-dimensional $S = 1$ array, and antiferromagnetic coupling

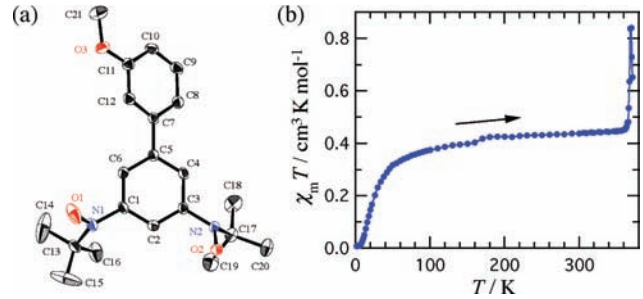

Figure 3. (a) X-ray crystal structure of 3MeOBPBN (296 K) with thermal ellipsoids at the 30% probability level. Hydrogen atoms have been omitted. Only the major conformer [0.72(3) occupancy] is shown for C14, C15, and C16. (b) Temperature dependence of $\chi_m T$ for 3MeOBPBN measured at 5000 Oe. A solid line is drawn as a guide for the eye.

occurs cooperatively at every N−O contacting site or at every two sites within a chain. The chain is not a simple $S = 1$ linear array, because the soft organic skeletons can accommodate the lattice distortion and modulate nearest-neighbor magnetic coupling.

In summary, we have clarified the gradual structural phase transition of crystalline 3MeBPBN by use of interactions varying in a spectrum from weak chemical bonding to strong antiferromagnetic coupling. The chromic and magnetic properties reversibly change in the solid state and irreversibly change at the melting point, and the transition temperature is sensitive to the steric effect.

Supporting Information Available: Crystallographic data (CIF) for 3MeBPBN (116 and 296 K) and 3MeOBPBN (296 K), tables of selected geometrical parameters, an animation of the phase transition of 3MeBPBN (QT), XRD results for 3MeBPBN, MO calculation results, molecular arrangements in the crystals, solution ESR spectra, and complete ref 3a. This material is available free of charge via the Internet at http://pubs.acs.org.

References

(1) *Spin Crossover in Transition Metal Compounds I, II, and III*; Gütlich, P., Goodwin, H. A., Eds.; Springer-Verlag: Berlin, 2004.
(2) Itkis, M. E.; Chi, X.; Cordes, A. W.; Haddon, R. C. *Science* **2002**, *296*, 1443. Fujita, W.; Awaga, K.; Matsuzaki, H.; Okamoto, H. *Science* **1999**, *286*, 261. Fujita, W.; Kikuchi, K.; Awaga, K. *Angew. Chem., Int. Ed.* **2008**, *47*, 9480.
(3) (a) Morita, Y.; et al. *Nat. Mater.* **2008**, *7*, 48. (b) Suzuki, S.; Morita, Y.; Fukui, K.; Sato, K.; Shiomi, D.; Takui, T.; Nakasuji, K. *J. Am. Chem. Soc.* **2006**, *128*, 2530.
(4) White, D. M.; Sonnenberg, J. *J. Am. Chem. Soc.* **1966**, *88*, 3825. Kishimoto, Y.; Abe, J. *J. Am. Chem. Soc.* **2009**, *131*, 4227.
(5) Hayashi, T.; Maeda, K. *Bull. Chem. Soc. Jpn.* **1960**, *33*, 565. Ohkanda, J.; Mori, Y.; Maeda, K.; Osawa, E. *J. Chem. Soc. Perkin Trans. 2* **1992**, 59.
(6) Kurokawa, G.; Ishida, T.; Nogami, T. *Chem. Phys. Lett.* **2004**, *392*, 74.
(7) Nishimaki, H.; Mashiyama, S.; Yasui, M.; Nogami, T.; Ishida, T. *Chem. Mater.* **2006**, *18*, 3602.
(8) Iwamura, H. *Adv. Phys. Org. Chem.* **1990**, *26*, 179. Rajca, A. *Chem. Rev.* **1994**, *94*, 871. Ishida, T.; Iwamura, H. *J. Am. Chem. Soc.* **1991**, *113*, 4238. Mukai, K.; Nagai, H.; Ishizu, K. *Bull. Chem. Soc. Jpn.* **1975**, *48*, 2381.
(9) Red plates. Mp: 77−79 °C. Anal. Found: C, 74.05; H, 7.98; N, 8.18. Calcd: C, 74.08; H, 8.29; N, 8.23 for $C_{21}H_{28}N_2O_2$. IR (KBr disk): 2974, 1595, 1574, 1448, 1180, 795, 704 cm^{-1}. ESR (X-band, toluene, room temperature): $g = 2.0060$, $\Delta B_{p-p} = 2.2$ mT (see Figure 5Sa).
(10) Selected data: triclinic $P\bar{1}$; $a = 9.2411(5)$ Å, $b = 10.3875(2)$ Å, $c = 11.7540(5)$ Å, $\alpha = 110.621(4)°$, $\beta = 96.472(3)°$, $\gamma = 112.361(4)°$; $V = 936.09(9)$ Å^3; $Z = 2$; $d_{calc} = 1.208$ g cm^{-3}; μ(Mo Kα) = 0.078 mm^{-1}; $R_{int} = 0.070$; $R(F)$ [$I > 2\sigma(I)$] = 0.0595; $R_w(F^2)$ (all data) = 0.1195; $T = 116$ K; 4175 unique reflections. For details, see the Supporting Information.
(11) Bondi, A. *J. Phys. Chem.* **1964**, *68*, 441.
(12) Red plates. Mp: 91−92 °C. Anal. Found: C, 70.76; H, 7.92; N, 7.86. Calcd: C, 70.68; H, 7.75; N, 7.80 for $C_{21}H_{28}N_2O_3$. IR (KBr disk): 2974, 1574, 1458, 1286, 1234, 1167, 1045, 787, 700 cm^{-1}. ESR (X-band, toluene, room temperature): $g = 2.0061$, $\Delta B_{p-p} = 2.3$ mT (see Figure 5Sb).
(13) Selected data: FW 356.45; triclinic $P\bar{1}$; $a = 9.747(4)$ Å, $b = 10.219(4)$ Å, $c = 11.139(4)$ Å, $\alpha = 83.48(4)°$, $\beta = 100.08(3)°$, $\gamma = 114.46(3)°$; $V = 993.3(7)$ Å^3; $Z = 2$; $d_{calc} = 1.192$ g cm^{-3}; μ(Mo Kα) = 0.080 mm^{-1}; $R_{int} = 0.050$; $R(F)$ [$I > 2\sigma(I)$] = 0.0676; $R_w(F^2)$ (all data) = 0.1111; $T = 296$ K; 4527 unique reflections. The cell was transformed for comparison with those of 3MeBPBN. For details, see the Supporting Information.

JA102890G